

# 24 $\mu$ Watt 26m Range Batteryless Backscatter Sensors with FM Remodulation and Selection Diversity

Georgios Vougioukas and Angelos Bletsas

School of Electrical and Computer Engineering, Technical University of Crete, Chania 73100, Greece

**Abstract**—Reflection radio principles, used in RFID systems, have been recently exploited in wireless sensor networking, due to their inherent low-power requirements. This work offers a complete batteryless analog sensor design, implemented and tested in real-world conditions, able to backscatter its sensed information, without any type of analog-to-digital converter (ADC), digital logic or dedicated illuminator, towards any off-the-shelf FM receiver. Selection diversity exploited simultaneous illumination from multiple FM broadcasting stations, located 6.5 km away. Sensor-to-smartphone distance of 26 and 15 meters, outdoors and indoors, respectively, was experimentally demonstrated at (audio) output SINR of 10 dB. The ultra-low cost circuit consumed measured power of 24  $\mu$ Watt in *continuous* and batteryless operation, tested with various ambient power sources. The design can in principle accommodate various resistive or capacitive sensors that can be literally “listened” by a single, conventional FM receiver (e.g., in a smartphone).

## I. INTRODUCTION

Apart from RFID applications, reflection radio principles have been recently exploited in wireless sensor networking, due to their inherent low-power requirements [1]. Energy is only needed for a switch that changes the load connected to an antenna, so that impinged RF signal is modulated by the tags’ antenna-load system. Thus, the communication energy and monetary cost per tag/sensor can be reduced, compared to conventional, Marconi radios.

However, an illuminating signal is required, as well as a *sensitive* receiver for the backscattered information. Work in [2], [3], [4] studied bistatic, digital, non-coherent communication with on-off keying (OOK) or frequency shift keying (FSK) modulation at the tag, also demonstrating extended communication ranges with software-defined radio (SDR) and semi-passive tags. Work in [5] demonstrated reception of bistatic backscatter radio with envelope detection, when the illuminating signal was also modulated, coming from a digital television (DTV) broadcaster.

Examples of analog bistatic backscatter communication are offered in [6], [7], [8]. These works described analog sensors backscattering information related to electric potential across the stem of a plant [6], environmental humidity [7], and soil moisture [8] using backscatter frequency modulation (FM), with a dedicated (illuminating) carrier emitter and a software defined radio as receiver.

Work in [9] exploited a FM broadcasting station as the illuminator.<sup>1</sup> The scatter radio tag consisted of an audio signal-controlled FM modulator, alternatively connecting the tag

<sup>1</sup>This work was implemented independently of [9]. While having finished the results and writing this paper, we run into that important piece of work.

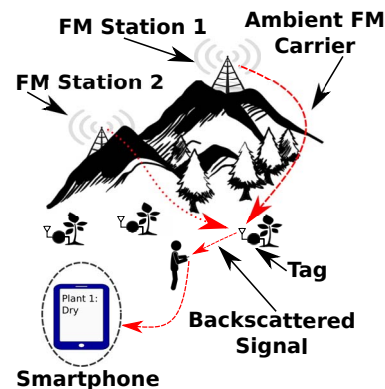


Fig. 1: Remodulation with backscatter and selection diversity.

antenna between two loads. The FM modulator was a signal generator in FM modulation mode, with input coming from a digital-to-analog converter, connected to a computer. The authors exploited 2, 16 audio tones or an (analog) audio signal from the tag/PC for (digital) 2-FSK, 4-FSK or analog backscatter communication, respectively, towards a conventional FM receiver. Tag-to-FM receiver ranges up to 60 ft were demonstrated with the above setup, while an integrated circuit, including digital logic that could replace the above tag/pc, was simulated. In contrast to prior art, the contributions of this work are summarized as follows:

- 1) This work offers a complete analog sensor design, implemented and tested in real-world conditions using off-the-shelf components, able to backscatter its sensed information, without any type of analog-to-digital converter (ADC) or digital logic, towards any off-the-shelf FM receiver (including those found in smartphones), exploiting as illuminators the FM broadcasting stations.
- 2) The ultra-low cost circuit consumed measured power of 24  $\mu$ Watt in *continuous* operation and was tested in batteryless operation with various ambient power sources (e.g., solar, ambient light with panel, photodiode, respectively or electrochemical energy from two lemons).
- 3) Selection diversity was exploited, given the fact that scatter radio modulation from the tag signal on the illuminating signal occurs at passband, and thus, tag signal is *simultaneously* modulated on *all* FM stations’ broadcasting signals. With careful exploitation of selection diversity, sensor-to-smartphone reception outdoor distance was experimentally measured at 26 meters

with audio output signal to interference plus noise ratio (SINR) of 10 dB.

- 4) The design can accommodate various resistive or capacitive sensors that can be received by a single, conventional FM receiver. Moreover, simple frequency division multiple access techniques can allow for simultaneous operation of multiple such tags.

Section II offers the basic principles of scatter radio FM remodulation and selection diversity, Section III describes the implementation, including measured power consumption of the implemented circuit, Section IV offers the experimental range results with/without selection diversity using a smartphone, and finally work is concluded in Section V.

## II. THEORY OF OPERATION

### A. Communication by means of reflection

Consider the case of a RF wave produced by a source with impedance  $Z_{\text{source}}$ . The source is connected to a load,  $Z_{\text{load}}$ . If the load is not matched with the source, i.e  $Z_{\text{source}} \neq Z_{\text{load}}^*$ , a portion of the power destined for the load will be reflected back to the source. The amount of reflection depends on the *reflection coefficient*, defined as:

$$\Gamma = \frac{Z_{\text{load}} - Z_{\text{source}}^*}{Z_{\text{load}} + Z_{\text{source}}}. \quad (1)$$

The above fact can be exploited to achieve communication. If the RF source is an antenna and a load is chosen in order to end up with reflection of the incident wave, the antenna is forced to reflect. On the other hand, if the load is matched to the antenna, ideally, the load absorbs all the power and no reflection occurs. By carefully choosing the loads and the alternation between them, we can manipulate the reflected signal to attain certain characteristics.

A system/tag comprised of an antenna terminated, alternatively, at two different loads  $Z_0, Z_1$  (resulting to  $\Gamma_0, \Gamma_1$ , respectively), using a RF switch is considered. The switch is driven by a square wave,  $s(t)$ , with frequency  $F_{\text{sw}}$  and 50% duty cycle. By keeping only the fundamental frequency component of  $s(t)$  (which holds  $\approx 80\%$  of  $s(t)$ 's power), the signal driving the switch can be expressed as:

$$x_{\text{sw}}(t) = A_{\text{sw}} \cos(2\pi F_{\text{sw}} t), \quad (2)$$

where in Eq. (2) a constant term related to the RF parameters of the system and the random phase in the cosine term have been ignored [4], for simplified explanation. It can be shown [4] that if the antenna of the aforementioned setup is illuminated by a high frequency signal  $c(t)$ , the signal backscattered from the antenna is given by:

$$y(t) = \sqrt{\eta} c(t) x_{\text{sw}}(t) = \sqrt{\eta} c(t) A_{\text{sw}} \cos(2\pi F_{\text{sw}} t), \quad (3)$$

where  $\eta$ , is the *scattering efficiency*, depending on the chosen loads and the antenna characteristics. It can be seen, from Eq. (3), that by alternating the termination of an antenna illuminated by  $c(t)$ , we get a modulation-like operation of the low frequency  $x_{\text{sw}}(t)$  signal, by the higher frequency  $c(t)$  signal.

### B. FM remodulation

The signal model of any  $\phi_s(t)$  that undergoes frequency modulation, is given by [10]:

$$c_s(t) = A_s \cos\left(2\pi F_s t + 2\pi k_s \int_0^t \phi_s(\tau) d\tau\right), \quad (4)$$

where  $A_s, F_s$  is the carrier amplitude and center frequency, respectively and  $k_s$  is the modulator's frequency sensitivity, measured in Hz/V. FM modulation index is given by  $\beta_s = \Delta f_{\text{max}}/W = k_s \max|\phi_s(t)|/W$ , where  $W$  is the (baseband) bandwidth of  $\phi_s(t)$ . If  $\max|\phi_s(t)| = 1$ , then  $\Delta f_{\text{max}} = k_s$ . Signal model in Eq. (4) applies to any FM radio station and thus,  $\phi_s(t)$  includes station's audio information (mono or stereo) plus any additional digital information about the station (RDS), when RDS is also transmitted.

If in Eq. (3),  $x_{\text{sw}}(t)$  admits the following form:

$$x_{\text{sw,FM}}(t) = A_{\text{sw}} \cos\left(2\pi F_{\text{sw}} t + 2\pi k_{\text{sw}} \int_0^t \mu(\tau) d\tau\right), \quad (5)$$

which means that the RF switch is driven by a square wave with fundamental frequency modulated by  $\mu(t)$  and the illuminating carrier is a *modulated* signal from a FM radio station (Eq. (4)), then the backscattered signal from the tag is given by:

$$\begin{aligned} y_{\text{bs}}(t) &= \sqrt{\eta} c_s(t) x_{\text{sw,FM}}(t) \\ &= \frac{\gamma_s}{2} \cos(2\pi (F_s + F_{\text{sw}}) t + \Phi_s(t) + \Phi_{\text{tag}}(t)) + \\ &\quad + \frac{\gamma_s}{2} \cos(2\pi (F_s - F_{\text{sw}}) t + \Phi_s(t) - \Phi_{\text{tag}}(t)), \end{aligned} \quad (6)$$

where  $\gamma_s = \sqrt{\eta} A_s A_{\text{sw}}$ ,  $\Phi_s(t) = 2\pi k_s \int_0^t \phi_s(\tau) d\tau$  and  $\Phi_{\text{tag}}(t) = 2\pi k_{\text{sw}} \int_0^t \mu(\tau) d\tau$ . Eq. (6) offers the sum of two FM signals, one at  $F_s + F_{\text{sw}}$  and another at  $F_s - F_{\text{sw}}$ , since their instantaneous frequency depends on  $\phi_s(t)$ ,  $\mu(t)$ . Thus, backscattering results to FM signaling when the illuminating signal is FM and the switching signal is also FM; such operation may be coined as *FM remodulation*. Notice that the FM signal at  $F_s \pm F_{\text{sw}}$  is attenuated by  $\sqrt{\eta}$ , while it contains information from both the FM station (which transmits at center frequency  $F_s$ ) and the tag. For the special case of  $\Phi_s(t) = \text{constant}$ , the above signal model is simplified to the bistatic scatter radio case, where the illuminating signal is an unmodulated carrier (as in e.g., [2]).

The FM remodulation principle observed above means that any conventional FM radio receiver, tuned at either of  $F_s \pm F_{\text{sw}}$ , can demodulate the backscattered signal, as long as the following conditions hold:

- 1)  $\mu(t)$  bandwidth is limited to the audible spectrum (20 Hz to 20 kHz) or up to the maximum frequency of 53 kHz (assuming stereo FM reception) or slightly above (including the band for RDS information).
- 2) At least one of  $F_s \pm F_{\text{sw}}$  falls within the FM radio frequency band (88 MHz to 108 MHz),
- 3) Audio level of the backscattered demodulated tag signal (given that it's limited to the audible spectrum) is above

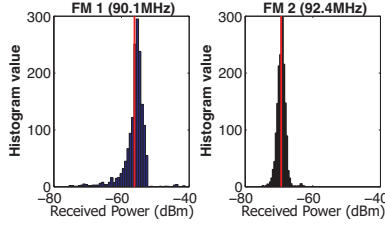


Fig. 2: Measured received power histogram at tag location from 2 NLOS FM stations, 6.5 km away from the tag.

a required threshold for successful FM reception. Note that  $\phi_s(t)$  acts as interference in the reception of  $\mu(t)$ .

In this work, sensor's  $\mu(t)$  is limited in the audible spectrum, potentially amenable to FM station's interference, while  $k_{sw} \neq k_s$ . To reduce interference from the FM station signal on the tag backscattered signal, the frequency band of  $\mu(t)$  may be placed on areas that are not occupied by frequency components of  $\phi_s(t)$ . For example, if the chosen FM radio station has only voice content,  $\mu(t)$  can be designed to occupy a higher frequency band. Additionally, experiments have shown that by increasing the frequency deviation of the switching signal (up to a certain value, so that the FM threshold phenomenon does not kick in), higher audio levels of  $\mu(t)$  are offered compared to interference. Such method does not eliminate interference but reduces its effect, allowing for successful sensor interrogation.

An alternative solution would be to demodulate and recover in parallel  $\phi_s(t)$ , using a SDR receiver or a second FM receiver and then perform interference cancellation. In this work, reception of the sensor's information is restricted to a single handheld smartphone with a single FM receiver.

### C. Ambient Selection Diversity

One of the beauties of backscatter radio is the fact that modulation is facilitated at *passband* and not at baseband, as in conventional Marconi radios; thus, sensor's switching according to Eq. (5) offers remodulated backscattered signal at  $\{F_s \pm F_{sw}\}$ , for all FM stations  $s \in \{1, 2, \dots, L\}$ . Thus, an immediate question arises: which FM station  $s \in \{1, 2, \dots, L\}$  should the handheld FM receiver select to tune at  $F_s \pm F_{sw}$ ? For  $L$  FM stations, there are  $2L$  possible passband frequencies for the smartphone FM receiver to select from. Fig. 2 offers the histogram of the received power from 2 non-line of sight (NLOS) FM radio stations, 6.5 km away, using a commercial portable spectrum analyzer (measurements every 2 sec for a duration of 1 hour for each station). It can be observed that the expected received power (reported by the vertical line) varies significantly ( $-56$  dBm vs  $-69$  dBm) among the two stations, while a similar observation holds from the standard deviation.

Selecting the FM station with the strongest received power, could increase the value of  $\gamma_s$  in Eq. (7), which is important, given that backscatter communications are link-budget-limited (i.e., noise limited) and higher carrier amplitude in FM modulation results to smaller impact of thermal noise at the

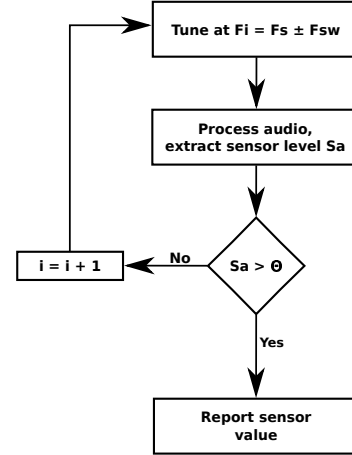


Fig. 3: Maximizing sensor's *audio output* level.

receivers' output. It is assumed that the impinging power at the tag antenna from station  $s \in \{1, 2, \dots, L\}$  is a Gamma-distributed random variable  $\gamma_s$  with shape and scale parameters  $k_s, \theta_s$ , respectively and the received power at the smartphone is also a Gamma-distributed random variable  $\gamma_0$  with shape and scale parameters  $k_0, \theta_0$ ; the latter two parameters incorporate, through the expected value, the tag fixed scattering efficiency  $\eta$ , as well as link-budget average loss due to tag-to-smartphone distance  $d_0$ . The following proposition holds for the end-2-end received power  $\gamma_s \gamma_0$  of the backscattered signal at the smartphone, under selection diversity among  $L$  potential FM stations:

**Proposition 1.** For  $\gamma_i \sim \text{Gamma}(\cdot; k_i; \theta_i)$ ,  $i \in \{0, 1, \dots, L\}$ , the benefits of selection diversity can be assessed by the following outage probability:

$$\Pr\left(\max_{i \in \{1, 2, \dots, L\}} \gamma_i \gamma_0 < \Theta\right) = \frac{1}{\theta_0^{k_0}} \frac{1}{\prod_{j=0}^L \Gamma(k_j)} \int_0^{+\infty} x^{k_0-1} e^{-\frac{x}{\theta_0}} \prod_{i=1}^L \gamma\left(k_i, \frac{\Theta}{\theta_i} x\right) dx \quad (8)$$

where  $\gamma(s, x) = \int_0^x t^{s-1} e^{-t} dt$  is the lower incomplete gamma function  $\Gamma(s) = \int_0^{+\infty} t^{s-1} e^{-t} dt$  the Gamma function and  $\Theta$  is a test (fixed) threshold value. The above probability decreases with increasing  $L$ .

Nevertheless, the above selection process is not sufficient. The above assume that there is no *other* interfering signal (e.g., from another FM station) at frequencies around  $F_s \pm F_{sw}$ . Additionally, the above selection does not necessarily minimize the interference from each FM station's own  $\phi_s(t)$  signal on the tag's signal  $\mu(t)$ .

Thus, an alternative is to select FM station  $s^*$ , where the demodulated sensor's audio signal level is maximized. That can be easily and directly implemented with a single smartphone FM receiver, tuning at  $2L$  frequencies  $F_s \pm F_{sw}$ ,  $s \in \{1, 2, \dots, L\}$  for given  $F_{sw}$  and selecting  $s = s^*$ , where the sensor's (demodulated) signal tone power is above a user-defined threshold  $\Theta$ . In the experiments,  $\Theta$  was selected 10

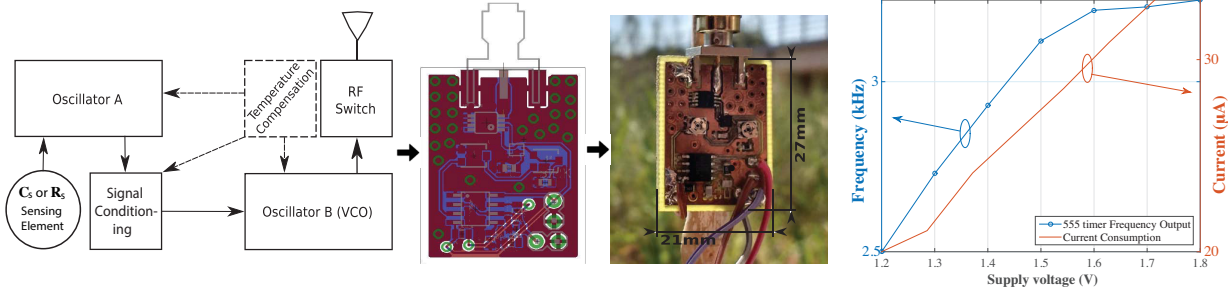


Fig. 4: Tag implementation & current consumption/frequency drift vs supply voltage.

dB above noise (thermal and interference) floor. Selecting the appropriate frequency  $F_i = F_{s^*} \pm F_{sw}$ , where the smartphone receiver should tune at (among  $2L$  candidates  $\{F_s \pm F_{sw}\}$ ,  $s \in \{1, 2, \dots, L\}$ ), so that receiver output level at sensor's expected audio band is maximized, is depicted in Fig. 3.

#### D. Multiple Access

One way for simultaneous operation of multiple, continuous backscattering sensors is to allocate the audible spectrum with non-overlapping frequency bands among the various sensors, by carefully tuning the circuit producing  $\mu(t)$  (discussed in Sec. III-A). A second more efficient way is to uniquely allocate, distinct center switching frequencies  $F_{sw}$  and frequency bands around them, among the sensors. Both ways above, essentially offer frequency division multiple access (FDMA), the first using the audible spectrum and the second using FM passband (from 88 MHz to 108 MHz). FDMA techniques have been already demonstrated experimentally in scatter radio networking (e.g., in [7]). A third way is to combine the above and a fourth way is combining time and frequency division multiple access techniques.

### III. IMPLEMENTATION

The basic tag/system idea is to design two oscillators, with the first producing sensor's modulating signal  $\mu(t)$  (1st modulation level) and the second be driven by the first (2nd modulation level), in order to produce the FM tag signal (according to Eq. (5)) to be scattered back. A capacitive  $C_s$  or resistive  $R_s$  sensing element is assumed, connected to the first oscillator, as shown in Fig. 4-left. In principle, any capacitive or resistive sensing element can be utilized, as explained below. Experiments have been conducted with two different capacitive sensing elements, one for soil moisture and another for air humidity.

#### A. Sensing Capacitor & Control Circuit

1) *1st modulation level:* Oscillator A is implemented with an ultra low power 555 timer, configured in astable mode, producing  $\mu(t)$  as a square pulses signal; its fundamental frequency and duty cycle are determined by external components, including the value of the utilized sensors' capacitance. As discussed in Section II-B, the circuit must be designed so that regardless of the sensor's value,  $\mu(t)$  will be always audible.

Thus, *any* sensing capacitor can be used with the circuit, as long as the design guarantees that the output will remain audible throughout the sensor's range. In this work, a soil moisture capacitor, part of the sensor in [8], [11] was used. An environmental humidity sensing capacitor (HCH-1000), part of the sensor in [7], [12] was also tested.

2) *2nd modulation level:* Oscillator B is implemented with a Silicon Laboratories TS3002 oscillator/timer, configured as a Voltage Controlled Oscillator (VCO) (Fig. 4-left). VCO's control voltage is set to be  $\mu(t)$ , effectively FM modulating  $\mu(t)$ . The maximum and minimum value of  $\mu(t)$  define the maximum and minimum frequency values produced by the VCO, which must also adhere to the required FM frequency deviation. VCO produces FM signal with specific frequency limits/deviation; this is accomplished by scaling  $\mu(t)$  with a signal conditioning block (Fig. 4-left), comprised of a resistor network.

Although not included in the present design, temperature compensation must be implemented. One way to compensate the change in resistors' values due to temperature variations is by using thermistors. Another way is to fully characterize tag's behavior with respect to temperature and then apply a correction on the measurement received by the reader. A combination of the two methods is also possible.

#### B. RF-switch

The Analog Devices ADG919 was chosen due to its ultra low power consumption ( $< 1\mu A$ ). According to datasheet, its minimum operating voltage is 1.65 V. Due to the ultra low power requirements of the overall tag, the switch was tested for operating *below* its stated minimum voltage. A VNA stimulated the switch with a signal at frequency 90 MHz, power  $-10$  dBm and the reflection coefficients  $\Gamma_0, \Gamma_1$  were measured. For supply voltage 1.2 V,  $|\Delta\Gamma|_{1.2V} \triangleq |\Gamma_1 - \Gamma_0| = 1.70$  and for 1.7 V,  $|\Delta\Gamma|_{1.7V} = 1.78$ . Ignoring the expected backscattering performance degradation, the switch operates even @ 1.2 V.

#### C. Power Consumption & Supply

For fixed sensing capacitor value (sensor dry), Fig. 4-right offers total current consumption of the overall tag, as a function of supply voltage; it is clearly shown that the system is capable of achieving  $< 20 \mu A$  @ 1.2 V, resulting

to  $24 \mu\text{W}$  of power consumption, even in *continuous* (non-duty cycled) operation. For fixed Oscillator A output frequency (using a standard capacitor as sensor), Fig. 4-right also offers the dependence of oscillator’s A fundamental frequency on supply voltage, directing the utilization of a voltage regulator, also discussed below. To showcase the ultra low power consumption of the proposed tag system, three experiments were conducted:

1) *Batteryless tag with photodiode*: The tag was tested using a Texas Instruments BQ25504 harvesting IC along with a BPW34 photodiode, as the harvesting element. The photodiode was exposed to the flashlight of a smartphone for  $\approx 6$  seconds. Then, the IC activated the tag, which was able to work for approximately the same amount of time. This time is more than enough to get a valid reading on the smartphone. Other energy harvesting methods can be used.

2) *Batteryless tag with solar panel*: A  $31 \times 31$  mm solar panel was used to power the tag. Under full sunlight conditions the panel was measured to provide short-circuit current  $I_{sc} = 40$  mA and open circuit voltage  $V_{oc} = 2.3$  V. The inherent solar panel output voltage variations could also cause large deviations on the received sensor value, according to Fig. 4-right. Instead of a maximum power point tracking circuit (not needed due to tag’s ultra low consumption), a 1.8 V voltage reference was used to provide stable supply voltage to the tag and the setup was tested outside (Fig. 5-left). The soil moisture sensor was placed on the soil of a flowerpot and while watering the flower, the expected audio frequency drop was observed in the smartphone.

3) *Batteryless tag with lemons*: The solar panel of the previous setup was replaced by two lemons. Each “battery” comprised of a lemon with two inserted electrodes. Electrode 1 was a zinc-plated nail and electrode 2 was a thick copper wire. Each lemon offered  $V_{oc} \approx 0.9$  V and  $I_{sc} \approx 600 \mu\text{A}$ . The two were connected in series to provide enough voltage, while the voltage reference was omitted. The same test was conducted as with the solar panel experiment above. It is noted that in the last two experiments (solar panel & lemons), the tag was supplied with 1.79 V and consumed  $32 \mu\text{A}$ . All the current and voltage measurements were made using a HP 34401A multimeter.

#### D. Receiver

As stated in Sec. II-B, any conventional FM radio receiver can be used, provided that  $\mu(t)$  is audible. The following options are readily available:

1) *Smartphone*: A large number of smartphones is equipped with FM radio. Exploiting selection diversity and tuning at the FM station that offers the strongest demodulated tag’s tone, the sensor’s value can be extracted by frequency estimation of the tag’s received audible tone; frequency estimation can be conducted with maximum likelihood (ML) techniques on the audio samples, using periodograms. Fig. 5-right shows screen captures of an audio spectrum application running on a Motorola Moto G3, while the soil moisture sensor is being gradually submerged into a glass of water.

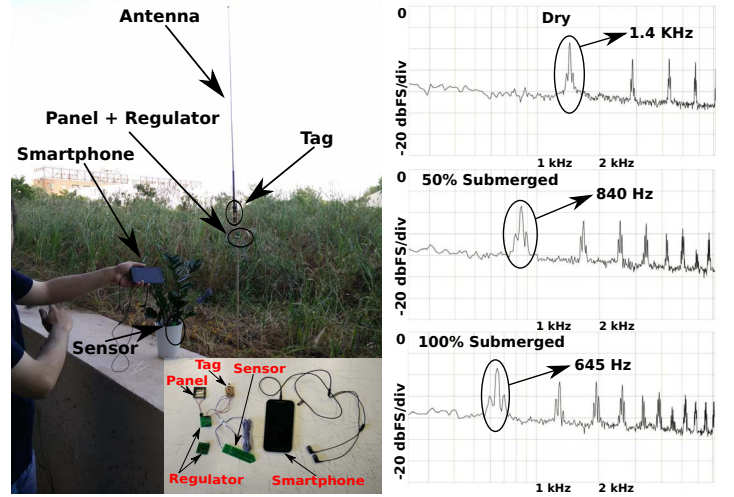


Fig. 5: Experimental setup using solar panel as power supply (left) and measured spectrum of smartphone audio output (right); the tag sensing capacitor is being gradually submerged in a glass of water (right).

The experiment was conducted indoors, with tag supplied at 1.2 V and tag-smartphone distance of 1 m. Clearly, the water level can be detected.

2) *Computer*: If a computer (e.g., embedded microprocessor) is needed to read the sensor, two options are offered. First, any conventional FM radio receiver can be connected to the computer’s audio in/microphone input. Alternatively, a software-defined radio (SDR) receiver, such as a RTL dongle, can be tuned at the FM band, perform demodulation, process the audio samples and recover sensor’s information as described above.

Second, a dedicated carrier, other than the ambient FM signals, can illuminate the tag. As described in Sec. II-B, the tag is indifferent with respect to the carrier used. A computer equipped with a SDR receiver can perform FM demodulation and recover the sensor’s value. To verify the last statement, experiments have been performed under illumination from a carrier on  $F_c = 868$  MHz. The receiver used was a low cost RTL dongle and the FM demodulation/sensor readout was performed in GNU radio. The only additional requirement of this technique is that tag’s antenna should be able to receive both at the FM as well as 868 MHz UHF band.

#### IV. OUTDOOR & INDOOR RESULTS

Range performance of the tag-smartphone system is tested in indoor and outdoor scenarios. The strength of the demodulated audio signal is reported, exploiting the Advanced Spectrum Analyzer PRO application, running at the smartphone. This application reports audio level in a scale of dBFS, which measures the audio level with respect to Full Scale audio input. Anything above  $-20$  dBFS is almost unbearable (using earphones) and anything below  $-70$  dBFS is noise. During the tests, a standard-value capacitor was utilized as the sensing capacitor, offering a fixed 1st modulation level

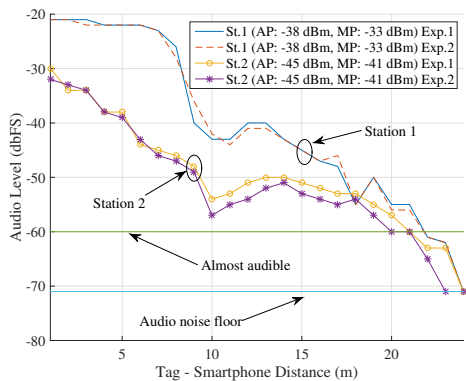


Fig. 6: Outdoor Performance, for 2 different radio stations. AP denotes the average power and MP the maximum.

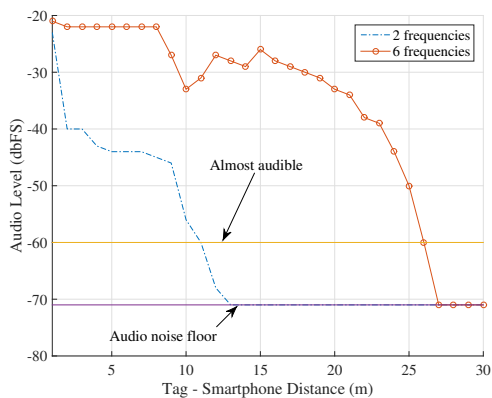


Fig. 7: Selection among up to 3 FM stations.

signal at frequency of 3.2 kHz. That was done to ease the process of acquiring measurements by ensuring a constant “sensor value” to be estimated at the smartphone/reader. It must be noted that, by choosing another signal frequency different performance results will be obtained. For the same reason, the tests were conducted using a 1.5V AA battery. The measurements reported audio level at 3.2 kHz, using the smartphone application’s markers. The power of FM stations’ received signal at the location of the tag was measured with a spectrum analyzer.

Outdoor performance results are offered for 2 FM stations in Fig. 6; it can be seen that the tag achieves at least **23 meters** before the audio tone power drops below  $-60$  dbFS, i.e., 10 dB above noise, resulting to demodulated backscattered signal SINR of 10 dB. The performance was tested for two different FM stations, offering different RF power levels; for each FM station, the test was repeated twice (Experiment 1 and 2) to showcase the slight variation in the measurements, due to wireless fading in the end-to-end link from FM station-to-tag-to smartphone. Indoor performance tests were performed in one of the department’s hallways. The communication range achieved was 15 meters exploiting an impinged power of  $-55$  dBm.

Finally, Fig. 7 repeats the same experiment as in Fig. 6 outdoors, where the smartphone chooses the frequency offering

the maximum audio level at the sensor’s tone among  $L = 3$  FM stations (i.e., the smartphone tunes at  $2L = 6$  frequencies and the strongest measurement is reported). The results show significant reception improvement, offering range up to 26 m. When selection is performed among two fixed frequencies, performance is weaker, highlighting again the importance of selection diversity; the latter comes for free for backscatter radio.

## V. CONCLUSION

This work presents a batteryless backscatter sensor circuit, able to be (literally) listened by any conventional FM radio receiver, including modern smartphones. Using a dedicated carrier emitter, in a bistatic topology is also possible, in conjunction with a computer and a SDR receiver. Experimental results showed that, under ambient FM illumination, the sensor’s value can be read even at distances of 15 and 26 meters for indoor and outdoor scenarios, respectively. The whole circuit consumption was measured at  $24 \mu\text{W}$  with continuous (non duty-cycled) operation. The design can accommodate various resistive or capacitive sensing elements. Benefits of selection diversity were also demonstrated, exploiting an inherent characteristic of scatter radio: modulation occurs at passband and thus, the tag signal *simultaneously* travels on several carriers.

## REFERENCES

- [1] G. Vannucci, A. Bletsas, and D. Leigh, “A software-defined radio system for backscatter sensor networks,” *IEEE Trans. Wireless Commun.*, vol. 7, no. 6, pp. 2170–2179, Jun. 2008.
- [2] J. Kimionis, A. Bletsas, and J. N. Sahalos, “Design and implementation of RFID systems with software defined radio,” in *Proc. IEEE European Conf. on Antennas and Propagation (EuCAP)*, Prague, Czech Republic, Mar. 2012, pp. 3464–3468.
- [3] —, “Bistatic backscatter radio for tag read-range extension,” in *Proc. IEEE RFID Technology and Applications (RFID-TA)*, Nice, France, Nov. 2012.
- [4] —, “Increased range bistatic scatter radio,” *IEEE Trans. Commun.*, vol. 62, no. 3, pp. 1091–1104, Mar. 2014.
- [5] V. Liu, A. Parks, V. Talla, S. Gollakota, D. Wetherall, and J. R. Smith, “Ambient backscatter: Wireless communication out of thin air,” in *ACM SIGCOMM*, Hong Kong, China, 2013, pp. 39–50.
- [6] C. Konstantopoulos, E. Kampianakis, E. Koutroulis, and A. Bletsas, “Wireless sensor node for backscattering electrical signals generated by plants,” in *Proc. IEEE Sensors Conf.*, Baltimore, MD, USA, Nov. 2013.
- [7] E. Kampianakis, J. Kimionis, K. Tountas, C. Konstantopoulos, E. Koutroulis, and A. Bletsas, “Backscatter sensor network for extended ranges and low cost with frequency modulators: Application on wireless humidity sensing,” in *Proc. IEEE Sensors Conf.*, Baltimore, MD, USA, Nov. 2013.
- [8] S. N. Daskalakis, S. D. Assimonis, E. Kampianakis, and A. Bletsas, “Soil moisture wireless sensing with analog scatter radio, low power, ultra-low cost and extended communication ranges,” in *Proc. IEEE Sensors Conf.*, Valencia, Spain, Nov. 2014, pp. 122–125.
- [9] A. Wang, V. Iyer, V. Talla, J. R. Smith, and S. Gollakota, “Fm backscatter: Enabling connected cities and smart fabrics,” in *USENIX Symposium on Networked Systems Design and Implementation*, Boston, MA, USA, Mar. 2017.
- [10] J. G. Proakis and M. Salehi, *Communication Systems Engineering*, 2nd ed. Upper Saddle River, NJ, USA: Prentice-Hall, 2001.
- [11] S. N. Daskalakis, S. D. Assimonis, E. Kampianakis, and A. Bletsas, “Soil moisture scatter radio networking with low power,” *IEEE Trans. Microwave Theory Tech.*, vol. 64, no. 7, pp. 2338–2346, Jul. 2016.
- [12] E. Kampianakis, J. Kimionis, K. Tountas, C. Konstantopoulos, E. Koutroulis, and A. Bletsas, “Wireless environmental sensor networking with analog scatter radio & timer principles,” *IEEE Sensors J.*, vol. 14, no. 10, pp. 3365–3376, Oct. 2014.